

## Optofluidic transport in liquid core waveguiding structures

Sudeep Mandal

*Applied and Engineering Physics, Cornell University, Ithaca, New York 14853*

David Erickson<sup>a)</sup>

*Sibley School of Mechanical and Aerospace Engineering, Cornell University, Ithaca, New York 14853*

(Received 16 March 2007; accepted 9 April 2007; published online 2 May 2007)

Here the authors introduce a method to achieve optofluidically based particle transport using liquid core waveguiding structures. Optically driven transport of 3  $\mu\text{m}$  polystyrene particles through a liquid core photonic crystal fiber is demonstrated and the resulting velocity distribution is characterized. The authors also show that dielectric particles can form highly concentrated bands within the liquid core with negligible transport based dispersion. They anticipate that this approach could lay the groundwork for an innovative class of optically driven particle concentration and separation devices. © 2007 American Institute of Physics. [DOI: [10.1063/1.2735560](https://doi.org/10.1063/1.2735560)]

The discovery that laser radiation could transfer its momentum to microscopic particles<sup>1</sup> and thus be used to manipulate them has led to many innovative applications for microscale total analysis systems. The recent interest in optofluidics<sup>2</sup> has led to a series of advanced implementations of various techniques to achieve all-optical control and sorting of particles into advanced and highly integrated microfluidic systems. They range from traditional optical tweezing,<sup>3</sup> rotational manipulation of components based on form birefringence,<sup>4</sup> to more recent electro-optic approaches such as that by Chiou *et al.*<sup>5</sup> Recently an optical force based cell sorting technique<sup>6</sup> was developed wherein rare cells were directed into separate streams following the detection of a green fluorescent protein at the interrogation site using radiation pressure. Although a variety of complex manipulations has been demonstrated,<sup>7</sup> most of them tend to be binary in nature, meaning that they can either trap or not trap a particle based on whether the conditions for trapping stability are met.<sup>8</sup> A number of studies have extended these ideas to exploit the dependence of this trapping potential on the particle properties, enabling much more advanced and subtle operations. For example, MacDonald *et al.*<sup>9</sup> demonstrated microfluidic sorting in a three dimensional optical lattice wherein particles of different sizes were sorted based on their differential affinity towards regions of high optical intensity. Imasaka<sup>10</sup> provided the initial foundation for optically driven separation techniques which he termed optical chromatography. In these systems the extreme sensitivity of the scattering force to particle size and refractive index (as will be described in greater detail below) is exploited to separate out inhomogeneous species from an initially mixed state. Recently pathogen detection using optical chromatography was demonstrated in a polydimethylsiloxane microfluidic system by Terray *et al.*<sup>11</sup> They demonstrated the separation of two closely related bacteria, *Bacillus anthracis* and *Bacillus thuringiensis*.<sup>12</sup> The noninvasive nature of these optical techniques makes them well suited for biomedical analysis devices.

At present one of the major limitations of these and other optically driven microfluidic systems is that the light-particle

interaction length is relatively small, limited by the focal depth of the free space optics. Since the spatial separation of optically different targets is proportional to the length of this interaction, this limits the efficiency with which precise separations can be conducted. Using a loosely focused beam increases the interaction length but requires much larger optical power to perform manipulations on these length scales. In this work we demonstrate optofluidically driven transport in liquid core waveguiding structures. Since the light remains confined within the liquid core, this gives direct access to the optical mode while increasing the light-particle interaction length by orders of magnitude. We have demonstrated that this allows for optically induced transport of microscopic particles over several centimeters, limited only by the optical power losses in the fiber.

Photonic crystal fibers (PCFs) guide light based on a photonic band gap effect.<sup>13</sup> In these devices a periodic lattice of air capillaries surrounds the core, creating a photonic band gap in the cladding which causes light of the wavelengths corresponding to this band gap to be confined within the low-index core. Here we extend previous works demonstrating particle levitation in air-core PCFs (Ref. 14) to liquid cores which enables bioanalytical functionality. To achieve light guidance we require the refractive index of the liquid core to be higher than the effective refractive index of the holey cladding region. This causes the light to undergo total internal reflection and thus remain confined within the liquid core. To create the desired refractive index contrast, we introduce the liquid in such a manner that it penetrates into the hollow core without penetrating into the capillaries (using a technique which will be described below).

A particle being guided through a liquid core PCF experiences four forces, namely, an axial scattering force  $F_{\text{scat}}$ , a gradient force  $F_{\text{grad}}$ , which can act in both the axial (due to losses along the length of the fiber) and radial directions (due to variations in the intensity profile), a gravitational force  $F_{\text{grav}}$ , and viscous drag  $F_{\text{visc}}$ . The origin of scattering and gradient forces lies in the change in momentum of the photons of the beam when they encounter the particle. The gradient force is proportional to the gradient of the field intensity, resulting in particles being pushed towards regions of higher optical intensity. In the limit of a Rayleigh particle transported in the low Reynolds number regime, it can be

<sup>a)</sup> Author to whom correspondence should be addressed; electronic mail: [de54@cornell.edu](mailto:de54@cornell.edu)

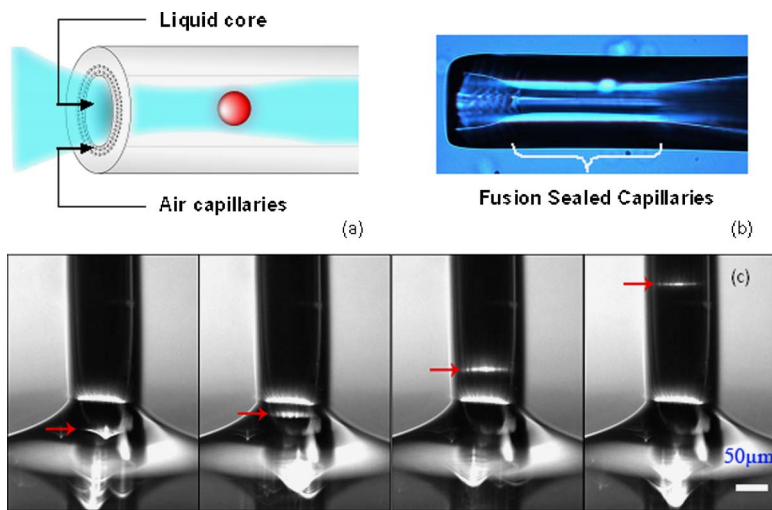


FIG. 1. (Color online) Optofluidic transport in a liquid core waveguiding structure. (a) Schematic illustrating optical excitation and transport of particles in the liquid core of a photonic crystal fiber. (b) Image of sealed air capillaries near the inlet of the fiber. (c) Detail of optically induced transport of  $3 \mu\text{m}$  polystyrene beads in the liquid core optical fiber near the inlet. Red arrow tracks a  $3 \mu\text{m}$  bead. Successive frames are spaced by 1 s.

shown (by equating the scattering and gradient force relations from Ashkin *et al.*<sup>15</sup> with Stokes drag) that the particle velocity  $v_p$  is

$$v_p(z) = \frac{64\pi^4 a^5 n_m \left( \frac{n_p/n_m}{2} - 1 \right)^2}{9\mu_m \lambda^4 c \left( \frac{n_p/n_m}{2} + 2 \right)} I(r, \theta, z) + \frac{a^2}{3c\mu_m} \left( \frac{n_p/n_m}{2} - 1 \right) \frac{\partial I(r, \theta, z)}{\partial z} - \frac{m_p g}{6\pi\mu_m a}, \quad (1)$$

where  $a$  is the particle radius,  $n_m$  and  $n_p$  are the medium and particle refractive indices,  $\mu_m$  is the viscosity,  $\lambda$  is the wavelength,  $c$  is the speed of light,  $m_p$  and  $g$  are the particle mass and gravitational acceleration, respectively, and  $I$  is the local intensity incident on the particle, which is in general a function of all three cylindrical coordinate directions. In Eq. (1) the first term is representative of the scattering force, the second of the gradient, and the third of gravity which, for our system, is oriented opposite the direction of the scattering force. From this expression it is evident that the propulsive velocity is extremely sensitive to the particle size ( $v \propto a^5$  in the scattering dominated limit) which compares extremely favorably with other bioanalytical separation techniques (the nearest competitor being dielectrophoresis which can be shown to have an  $a^2$  separation velocity dependence on particle size). From Eq. (1) it is apparent that a transported particle should come to rest at a location  $z$  where the scattering force is balanced by the gradient (which acts downwards since  $\partial I/\partial z < 0$  for a lossy fiber) and gravitational forces.

In the experiments conducted here we used a  $20 \mu\text{m}$  diameter core hollow-core PCF (Crystal Fiber, HC19-1550-01) as shown in Fig. 1. To selectively fill the hollow core with liquid we close the capillary ends at the fiber mouth while leaving the core open. To achieve this we evaluated UV curing<sup>16</sup> and fusion splicing techniques.<sup>17</sup> The latter technique (which was used here) was found to be more reliable. High temperatures during the fusion process cause the small capillaries to collapse into each other, while the central core remains largely unaffected due to its larger diameter. A 488 nm argon-ion laser beam is made incident on a  $4\times$  microscope objective to couple it into the fiber. The PCF is dipped in a glass container filled with a dilute aqueous solution of  $3 \mu\text{m}$  fluorescent polystyrene beads. A  $40\times$  objective at the other end of the fiber is used to image the near field pattern of the emerging laser beam. This is required to ensure that the light is being coupled into the core as slight mis-

alignments can lead to light coupling into the silica cladding. A charge coupled device camera with an attached microscope objective is used to image particles rising up the immersed tip of the fiber. Initially the fiber end was dipped in de-ionized water and the fiber was aligned so as to couple light into it. Once proper light guidance through the liquid filled core was confirmed, small quantities of  $3 \mu\text{m}$  fluorescing polystyrene particles were introduced into the water. As is shown in Fig. 1, particles in the path of the 488 nm laser beam were pushed axially upwards through the fiber end. The ultimate travel distance of the particles was strongly dependent on the quality of the optical coupling. In some cases we were able to transport particles over distances of greater than 2 cm with a laser excitation power of 210 mW (measured at the laser output).

To characterize the transport dynamics of the system a series of velocity measurements was performed in a different experiment, as shown in Fig. 2. The excitation laser power measured directly at the laser output was 120 mW. These measurements were made approximately  $100 \mu\text{m}$  from the mouth of the fiber. As can be seen the data set shows a near normal distribution in the velocity frequency centered around a median value of  $70 \mu\text{m/s}$ . Care was taken to ensure that the suspending fluid was quiescent during these measure-

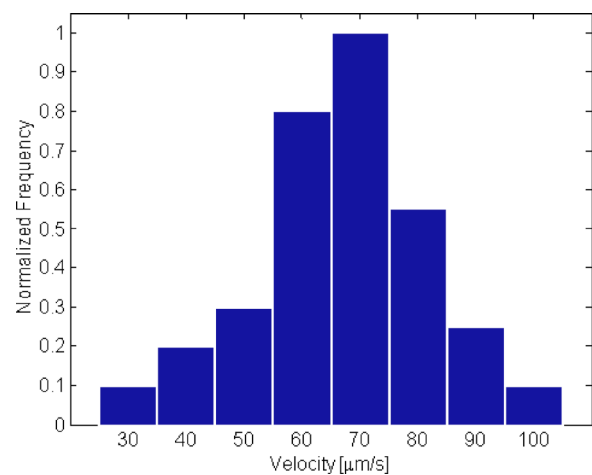


FIG. 2. (Color online) Experimentally measured particle velocity distribution. Transport velocities were measured for  $3 \mu\text{m}$  beads. As can be seen the velocity distribution showed a near normal distribution centered around  $70 \mu\text{m/s}$ .

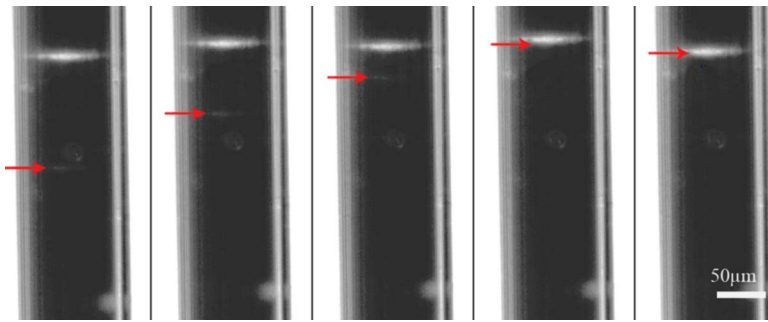


FIG. 3. (Color online) Formation of stable “floating bands” in liquid core. Demonstration of the concentration of particles into a stable band structure in a liquid core waveguiding structure. Red arrow tracks a  $3 \mu\text{m}$  bead. Successive frames are spaced by 66 ms and the input laser power was 210 mW. As can be seen the concentrated band shows almost no transport based sample dispersion. A video showing the transport and band formation is available from Ref. 18

ments, and thus the nonuniform distribution could not be the result of a parabolic flow profile bias, resulting from an induced pressure. The liquid core PCF is multimoded due to the large difference in refractive index between the core and cladding. Considerable mode hopping due to the liquid core and the particles propagating through the core was observed. We expect this mode hopping to be responsible for the measured velocity distribution.

We have also observed the concentration of similar  $3 \mu\text{m}$  polystyrene particles into distinct “floating bands” within the liquid core of the PCF.<sup>18</sup> An example is shown in Fig. 3 which tracks a single particle being attracted into such a band. This banding was demonstrated at excitation powers as low as 50 mW and it was observed that these bands can comprise an extremely large number of particles (no upper limit was detected here). The axial resting place of the floating band was shown to rise with increasing incident power and vice versa. As mentioned earlier, at a particular height the axial scattering force is exactly balanced by the weight of the particle and loss induced gradient force. As can be seen in Fig. 3 the observed bands are highly compact, exhibiting very little axial dispersion (spreading) which is counterintuitive given the spread in the transport velocity shown in Fig. 2. Mode hopping was also observed to vary the absolute location of the band along the transport axis but did not result in any observable dispersion. We believe that this antidispersive concentrating effect results from a sharp localized drop in the field intensity as a result of scattering at the band location. The resulting change in field intensity strongly enhances the local gradient force pulling particles into the formations while maintaining a strong scattering force acting from below.

Here we have illustrated an optofluidic technique for particle concentration and trapping. While others have demonstrated particle motion in photonic crystal fibers,<sup>14</sup> our work demonstrates optical transport in a liquid core waveguiding structure over long lengths, the spatial characterization of the transport velocities, and the optically in-

duced concentration of particles into discrete bands. The light-particle interaction length in our proposed technique is orders of magnitude larger than existing systems. This has great potential in optical chromatography systems for ultra-precise particle separations as well as in performing fluidic particle transport without flow field manipulations.

This work was partially supported by the U.S. National Science Foundation through the Sensors and Sensor Networks program under Grant No. NSF/CTS 0529045.

<sup>1</sup>A. Ashkin, *Phys. Rev. Lett.* **24**, 156 (1970).

<sup>2</sup>D. Psaltis, S. R. Quake, and C. H. Yang, *Nature (London)* **442**, 371 (2006).

<sup>3</sup>D. G. Grier, *Nature (London)* **424**, 810 (2003).

<sup>4</sup>S. L. Neale, M. P. Macdonald, K. Dholakia, and T. F. Krauss, *Nat. Mater.* **4**, 530 (2005).

<sup>5</sup>P. Y. Chiou, A. T. Ohta, and M. C. Wu, *Nature (London)* **436**, 370 (2005).

<sup>6</sup>M. M. Wang, E. Tu, D. E. Raymond, J. M. Yang, H. Zhang, N. Hagen, B. Dees, E. M. Mercer, A. H. Forster, I. Kariv, P. J. Marchand, and W. F. Butler, *Nat. Biotechnol.* **23**, 83 (2005).

<sup>7</sup>J. E. Curtis, B. A. Koss, and D. G. Grier, *Opt. Commun.* **207**, 169 (2002).

<sup>8</sup>A. Ashkin and J. P. Gordon, *Opt. Lett.* **8**, 511 (1983).

<sup>9</sup>M. P. MacDonald, G. C. Spalding, and K. Dholakia, *Nature (London)* **426**, 421 (2003).

<sup>10</sup>T. Imasaka, *Analisis* **26**, 53 (1998).

<sup>11</sup>A. Terray, J. Arnold, and S. J. Hart, *Opt. Express* **13**, 10406 (2005).

<sup>12</sup>S. J. Hart, A. Terray, T. A. Leski, J. Arnold, and R. Stroud, *Anal. Chem.* **78**, 3221 (2006).

<sup>13</sup>J. C. Knight, *Nature (London)* **424**, 847 (2003).

<sup>14</sup>F. Benabid, J. C. Knight, and P. Russell, *Opt. Express* **10**, 1195 (2002).

<sup>15</sup>A. Ashkin, J. M. Dziedzic, J. E. Bjorkholm, and S. Chu, *Opt. Lett.* **11**, 288 (1986).

<sup>16</sup>K. Nielsen, D. Noordegraaf, T. Srensen, A. Bjarklev, and T. P. Hansen, *J. Opt. A, Pure Appl. Opt.* **7**, 13 (2005).

<sup>17</sup>L. Xiao, W. Jin, M. Demokan, H. Ho, Y. Hoo, and C. Zhao, *Opt. Express* **13**, 9014 (2005).

<sup>18</sup>See EPAPS Document No. E-APPLAB-90-040718 for real time movie demonstrating the transport of  $3 \mu\text{m}$  beads in a liquid core photonic crystal fiber and the formation of a highly concentrated “floating band.” This document can be reached via a direct link in the online article’s HTML reference section or via the EPAPS homepage (<http://www.aip.org/pubservs/epaps.html>).